

1  
2  
3  
4  
5  
6  
7  
8  
9  
10  
11  
12  
13  
14  
15  
16  
17  
18  
19  
20  
21  
22  
23  
24  
25  
26  
27  
28  
29  
30  
31

## Subsurface Flow Batteries: Concept, Benefits and Hurdles

D Waltham<sup>1\*</sup>, K B Holt<sup>2</sup>, S Kuenzel<sup>3</sup>, A Basu<sup>1</sup>, N Lecoeur<sup>1</sup>

1. Department of Earth Sciences, Royal Holloway, Egham, Surrey TW20 0EX, UK

2. Department of Chemistry, University College London, London WC1H 0AJ, UK

3. Department of Electrical Engineering, Royal Holloway, Egham, Surrey TW20 0EX, UK

Email: [D.Waltham@rhul.ac.uk](mailto:D.Waltham@rhul.ac.uk)

**Abstract:** Storage of flow-battery electrolytes in aquifers is a novel concept for storing electrical energy in the subsurface. Flow-batteries operate by electrochemical transformations of electrolytes, rather than of electrodes, and their energy capacity can therefore be increased indefinitely by using larger electrolyte tanks. Saline aquifers may be the cheapest way to provide large-scale storage for this purpose. Storage would be within high-porosity, high-permeability reservoirs sealed by impermeable layers but—in contrast to hydrocarbon, H<sub>2</sub> or CO<sub>2</sub> storage—electrolytes would be trapped in lows (rather than highs) of such formations as a consequence of their high density compared to natural brines.

We investigate a range of electrochemical, geochemical, microbiological and engineering hurdles which must be overcome if subsurface flow-batteries are to become a practical technology. No insurmountable problems were found but further laboratory studies are needed. Our economic assessment suggests that subsurface flow batteries should be more cost effective than hydrogen-based power-to-gas approaches for discharge/charge timescales of around a day but that hydrogen will be cheaper for longer-term storage. Hence, meeting future energy-storage needs may involve a combination of both approaches.

A non-peer-reviewed preprint submitted to EarthArXiv. MS is in review for a Special Publication of the Geological Society of London.

32 **Introduction**

33 This paper considers a novel proposal for storage of electricity (specifically, storing electrochemically  
 34 active fluids—electrolytes—within subsurface, porous reservoirs). We begin by looking at why  
 35 energy needs to be stored at all so that we can discuss where our proposal might find a niche in the  
 36 spectrum of storage technologies.

37 The need for storage arises because electricity supply rarely matches demand. Demand fluctuates  
 38 through the day, as consumer and industrial needs cycle up and down, and fluctuates over the  
 39 seasons as the need for heating and cooling changes with the weather. Increasingly—as  
 40 intermittent, renewable energy generates a growing fraction of total electricity—supply also  
 41 fluctuates because the sun doesn't always shine and the wind doesn't always blow.

42 The supply/demand mismatch can occur on timescales from seconds to months and causes a range  
 43 of different problems summarised in Table 1 (adapted from Schmidt et al, 2019). The table consists  
 44 of rows showing different benefits of storage and columns showing different methods of storage. A  
 45 review of energy storage methods can be found in IRENA (2017). However, it is worth expanding on  
 46 the storage-benefits as this will assist our assessment of the new storage approach we propose in  
 47 this paper.

	Pumped Hydro	Compressed Air	Flywheel	Li-ion	Sodium-Sulphur	Lead Acid	Vanadium Flow	Hydrogen	Super capacitor
Frequency & voltage control			x	x	x	x	x	x	x
Load balancing	x	x	x	x	x	x	x	x	x
Peaker replacement	x	x		x	x	x	x	x	
Seasonal storage	x	x					x	x	
Congestion management	x	x		x	x	x	x	x	

48  
 49 Table 1. Reasons for balancing electricity supply/demand and technologies for achieving balance (adapted  
 50 from Schmidt et al, 2019)

51 The first four benefits are broadly given in order of increasing timescale. The timescale boundaries  
 52 between these benefits are arbitrary and blurred but it is nevertheless useful to divide them up in  
 53 this way. These benefits are:

- 54 i. Frequency and voltage instabilities occur almost instantly when supply does not match  
 55 demand. Handling this issue does not require large energy capacity but it does require a  
 56 rapid response within seconds.
- 57 ii. Load balancing refers to managing short term power mismatches on timescales of minutes.  
 58 On these timescales it is not possible to simply turn on and off additional generation  
 59 capacity (see peaker plants, below). Hence, approaches are required that respond and  
 60 provide/consume electricity on time scales longer than those used for frequency  
 61 stabilization but shorter than the time for peaker plant activation/deactivation.
- 62 iii. Peaker replacement refers to replacing "peaker plants" (currently usually medium sized gas-  
 63 fired turbines) that provide (relatively expensive) supplies when demand is high (e.g. for a  
 64 few hours in the evenings).
- 65 iv. Seasonal balancing is the issue of providing sufficient power to cope with higher demand on  
 66 timescales of weeks or months (e.g. for heating during winter).
- 67 v. Congestion management refers to longer term (hours to days) control of the consequences  
 68 of too much, rather than too little, energy supply. For example, on windy summer days there  
 69 may be more renewable energy than the grid requires. At present this is often managed by

70 closing down wind farms but this is not a good use of expensive infrastructure. Storage of  
71 the excess would be a better solution.

72 With this background it can be seen that some energy storage approaches (e.g. flywheels and  
73 supercapacitors) are more useful for rapid/low-capacity applications whilst others (e.g. CAES and  
74 PHS) are more useful for slow/high-capacity applications.

75 This paper's proposal, to store energy electrochemically in the subsurface, is likely to be similar to  
76 CAES, H<sub>2</sub> storage and PHS in terms of the speed with which it can be accessed. We'll also show, later,  
77 that it will be similar to PHS in terms of capacity. It is therefore useful to add a little more detail  
78 about the power and capacity of typical PHS storage as this is the approach that might be most  
79 directly replaced by electrolyte storage.

80 At present, most of the global electricity storage capacity is in the form of pumped hydroelectric  
81 storage. The largest existing PHS plant, in the UK, is the Dinorwig Power Station in north Wales with  
82 an energy storage capacity of 9.1 GWh at a maximum power of 1.7 GW (Scottish Renewables 2016).  
83 Hence, this system can store or release electricity, at maximum power, for  $9.1/1.7=5.4$  hours. The  
84 planned Coire-Glas PHS project in Scotland will have slightly lower power (1.5 GW) but a capacity of  
85 30-40 GWh (ibid) thus giving a discharge/charge time, at maximum power, of 20-27 hours.

86 However, PHS systems are confined to mountainous geographical locations which are often remote  
87 from electricity generators and users. Furthermore, building the numbers of PHS systems that will be  
88 required, as the renewable energy share of generation increases, is simply not practical. For  
89 example, the IEA (2009) projects that the need for additional electrical storage may be as high as  
90 90GW in Western Europe alone by 2050, i.e. 60 storage facilities as large as Coire-Glas. It is unlikely  
91 that enough suitable sites can be found and additional ways of storing electrical energy on PHS-like  
92 timescales will be needed.

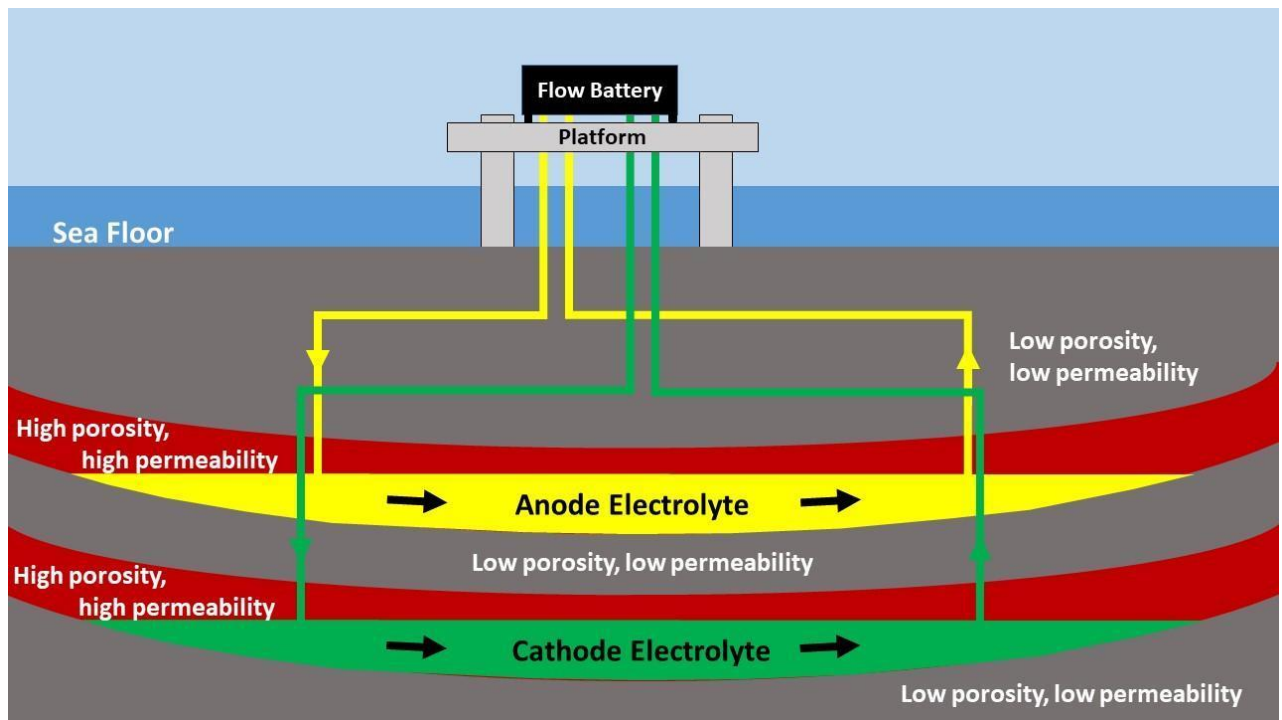
93 Subsurface hydrogen storage and/or compressed-air energy storage (CAES) may be good PHS  
94 replacements but this paper investigates, for the first time, whether subsurface flow batteries (SFBs)  
95 should also be considered.

96 Flow batteries differ from traditional batteries by using electrochemical transformations of (two  
97 separate) electrolytes rather than of electrodes (Park *et al.* 2016)(see later for more details). As a  
98 consequence, they can provide high energy-capacity at low cost if large, cheap electrolyte tanks are  
99 available. This paper considers whether porous-rock reservoirs are suitable storage locations (see  
100 Fig. 1). This concept of electrolyte storage in porous reservoirs is novel although energy companies  
101 are considering storage of electrolytes in salt caverns (EWE, 2017; RWE, 2020).

102 Within a porous reservoir, electrolytes would be pumped out at one end of their respective  
103 reservoirs, through the flow-battery and back into the opposite end of their reservoirs during  
104 charging. The flow direction would reverse during discharging. Hence, the volume of electrolyte in  
105 each reservoir would be kept constant (ignoring small changes in volume associated with chemical  
106 and physical alterations of the electrolytes).

107 The next section provides a brief introduction to flow batteries for the benefit of readers who may  
108 be unfamiliar with this technology. Then we look at the theoretical storage capacity and  
109 charge/discharge power that might be achieved by subsurface flow batteries. This is followed by a  
110 discussion of various electrochemical, geochemical, microbiological and engineering hurdles that  
111 must be overcome if SFBs are to become a practical technology. We finish with a look at costs

112 compared to other electrical storage technologies. Hence, this paper gives an initial assessment of  
113 whether SFBs could be technically, environmentally and economically viable.



114  
115 Figure 1. The subsurface flow-battery concept. Low-cost, high-capacity electrolyte storage is provided by  
116 porous reservoirs. Electrolyte density will be higher than that of natural brines and, hence, storage will be at  
117 the base of the reservoirs with an underlying “cap” rock.

118  
119 **Flow Batteries**

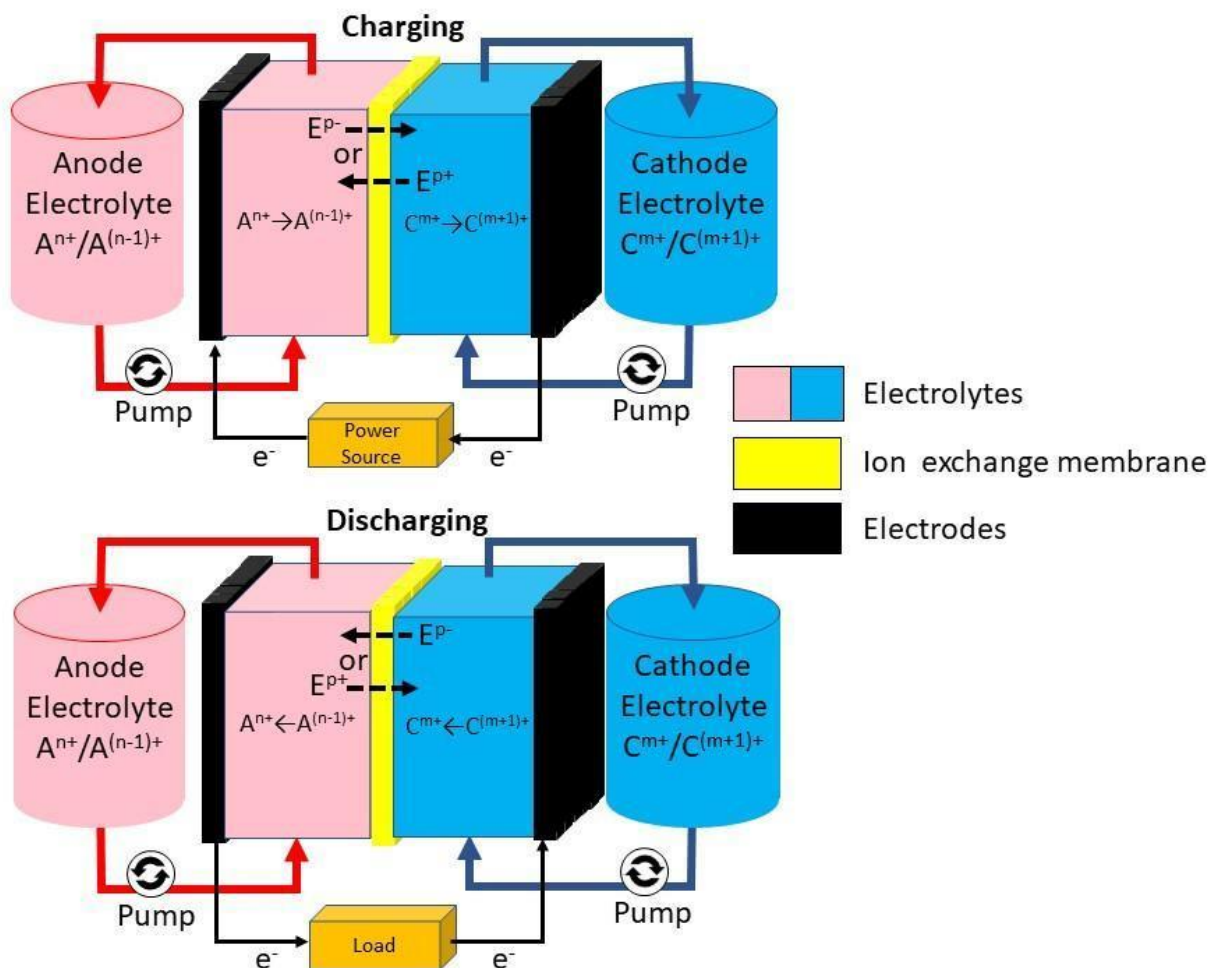
120 Flow batteries were first developed by NASA in the 1970s but they are not yet sufficiently  
121 widespread that we can assume familiarity outside the field of electrochemistry. Hence, we include a  
122 brief summary here. For further information, readers are directed to our main source for this  
123 overview (Weber, 2011).

124 As stated above, the key characteristic of flow batteries is that the electrochemical transformations,  
125 that generate and store electricity, take place in liquid electrolytes whilst the electrodes remain  
126 unaltered. Conventional batteries are the exact opposite; they involve chemical transformations of  
127 electrodes mediated by a passive electrolyte.

128 Figure 2 illustrates the generic operation of a rechargeable flow battery. Unlike a conventional  
129 battery, there are two distinct electrolytes, i.e. an anode electrolyte initially containing  $A^{n+}$  cations  
130 and a cathode electrolyte initially consisting of  $C^{m+}$  cations (where A and C are chemical species and  
131 m and n are small integers). The anode/cathode convention is potentially confusing in rechargeable  
132 batteries but, here, we use the convention that the cathode produces electrons during charging.

133 During charging, electron flow allows  $A^{n+} \rightarrow A^{(n-1)+}$  (by addition of electrons) and  $C^{m+} \rightarrow C^{(m+1)+}$  (by  
134 removal of electrons). Overall charge balance in the electrolytes is maintained by exchange of ions  
135 across a membrane. Exchange ions, E, can be negatively or positively charged and will flow from the  
136 anode to the cathode if negative, but from cathode to anode if positive. The transformations of A  
137 and C, and the flow of E across the membrane, are reversed if the battery is discharged rather than

138 charged. Note that, except when fully charged or discharged, the anode and cathode electrolyte  
 139 tanks contain a mixture of  $A^{n+}/A^{(n-1)+}$  and  $C^{m+}/C^{(m+1)+}$  respectively.

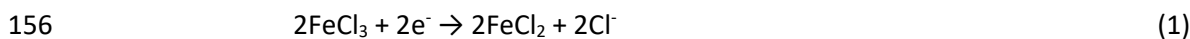


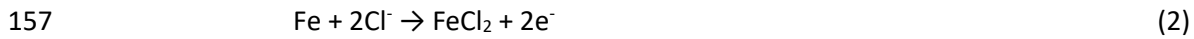
140  
 141 Figure 2. Operation and architecture of a generic flow battery. Upper diagram shows transformations and  
 142 ion/electron flow during battery charging. Lower diagram shows these reversed during discharging. See text  
 143 for further details.

144 The architecture of the flow battery consists of a “stack” (i.e. the central cell containing the  
 145 electrodes, membrane and reacting electrolytes) and external tanks containing the bulk of the  
 146 electrolytes. This architecture leads to the key benefit of the flow-battery design; it separates power  
 147 (rate of energy output or storage) from capacity (maximum amount of energy stored). Specifically,  
 148 the power of the system is increased by having more stacks (or a bigger membrane/electrode area in  
 149 the stack), whereas the capacity is increased by having larger external tanks.

150 The electrolytes must, of course, also contain cations (which may, or may not, be the same as the  
 151 exchange ions that cross the membrane). The resulting electrolytes can also be water based or use a  
 152 non-aqueous solvent. Hence—given the wide range of possible anions, cations, exchange ions and  
 153 solvents—flow batteries can be constructed using a large number of different chemical systems. In  
 154 this paper we concentrate upon the all-iron design of flow battery (Hruska and Savinell 1981).

155 The chemical reactions in the two halves of a discharging all-iron cell are





158 The first reaction occurs within a mixed  $\text{FeCl}_3/\text{FeCl}_2$  aqueous electrolyte whilst the second reaction  
159 involves dissolution of an iron-electrode into an  $\text{FeCl}_2$  aqueous electrolyte. The chloride ions  
160 generated in reaction (1) diffuse across the ion exchange membrane to provide the chloride ions  
161 consumed in reaction (2).

162 “All-iron” refers to having iron compounds in both halves of the cell (i.e. A and C in Fig. 2 are both  
163 iron species). This reduces the amount, and impact, of diffusion across the membrane of iron ions. In  
164 general, it is not possible to restrict ion exchange only to the desired exchange ions but exchange of  
165 any other electrolyte ions is undesirable as it reduces the recovered energy and alters electrolyte  
166 compositions.

167 Hruska and Savinell (1981) give the voltage of the resulting cell as 1.21V and estimate the charge  
168 density of the electrolyte at 63.5 Ah/l. Hence, the theoretical energy density is  $1.21 \times 63.5 = 76.8$   
169 Wh/l (or, equivalently,  $\text{kWhm}^{-3}$ ). This is probably close to the maximum upper limit since Hruska and  
170 Savinell (ibid) assumed a highly concentrated iron-chloride solution (500 g/l  $\text{FeCl}_3 \sim 6\text{M}$ ). Note that  
171 this concentration is four orders of magnitude higher than the median iron concentration of 21 mg/L  
172 (range 0.1 - 985 mg/L,  $n = 100$ ) reported in North Sea formation water (Warren et al., 1994). The  
173 energy density of the electrolytes is a key parameter since it will control the maximum amount of  
174 energy that can be stored in a reservoir of a given size and the maximum charge/discharge power for  
175 a given electrolyte pumping rate. We will put numbers on these quantities later in this paper.

176 An alternative all-iron design involves sulphate as the cation rather than chloride (Tucker et al, 2015;  
177 Yu et al 2021). This reduces problems with chlorides (principally highly corrosive electrolytes and  
178 problems with membrane longevity) but at the cost of lower-solubility and, hence lower  
179 concentration and energy density.

180 Note that, since the all-iron design involves dissolution and re-plating of an iron-electrode, it is a  
181 hybrid rather than pure flow battery. However, there are good reasons for choosing the all-iron  
182 configuration. Ferrous ions, sulphate ions and chloride ions are common constituents of subsurface  
183 brines (e.g. see Munz et al., 2010) and, hence, this particular flow battery chemistry is  
184 environmentally benign. Iron chlorides and sulphates are also low cost and widely available at  
185 industrial volumes. Iron chloride is particularly low cost as it is a by-product of the steel industry  
186 (Narayan et al, 2019).

187 Low cost and low environmental impact are our main reasons for focussing on the all-iron flow-  
188 battery in this preliminary assessment of SFBs. However most of our conclusions apply, or can be  
189 extended, to other flow battery designs. Common alternatives are an all-Vanadium design (the most  
190 technically developed flow battery at present but with expensive, toxic electrolytes), an iron-  
191 chromium design (which suffers from iron and chromium leakage across the membrane), a bromine-  
192 polysulphide design (which is prone to generating toxic  $\text{HS}$  and  $\text{Br}_2$  gases), zinc-bromine (with similar  
193 issues due to  $\text{HBr}$  and  $\text{Br}_2$ ) and a range of non-aqueous systems (which suffer from low electrolyte  
194 conductivity and high cost).

195

## 196 **Theoretical Subsurface Flow Battery Performance**

197 For illustrative convenience the two electrolytes in a subsurface flow battery are shown, in Fig. 1, as  
198 separated vertically. However, horizontal separation within multiple synclines of the same formation  
199 is also possible. The electrolytes will have high ion concentrations (compared to natural brines) in

200 order to store significant energy and, hence, they will be relatively dense and sink to the base of the  
 201 reservoir formation (as shown in Fig. 1). This leads to the first advantage of SFBs; electrolyte storage  
 202 will be in synclinal structures sealed by underlying low-permeability formations. In contrast, CO<sub>2</sub> and  
 203 H<sub>2</sub> subsurface storage are in anticlinal structures and so SFBs will not compete for the same storage  
 204 locations. Furthermore, accidental leakage can be contained simply by shutting the pumping system  
 205 down allowing dispersion of environmentally ubiquitous ions into the deeper subsurface.

206 However, SFBs are only useful if they can store/discharge electricity at high enough power.  
 207 Furthermore, if they are to be used for longer-term storage, they must have a large energy-storage  
 208 capacity. A combination of potential-flow theory and Darcy's law allows a first pass estimate of these  
 209 quantities. This approach has been widely used to model subsurface flows for many decades (e.g.  
 210 see King Hubbert, 1957).

211 Potential-flow theory assumes that slow, steady flows are irrotational and, hence, that velocity can  
 212 be represented as the gradient of a potential field, i.e.

$$213 \quad \mathbf{u} = \nabla\Phi \quad (3)$$

214 where  $\mathbf{u}$  is the flow velocity and  $\Phi$  is potential. The simplified case of simultaneous injection and  
 215 extraction of electrolyte using two perforated, vertical wells in a horizontal layer—of constant  
 216 thickness, porosity and permeability—can then be modelled as a 2-dimensional potential flow, from  
 217 a point source into a point sink, with a potential of

$$218 \quad \Phi = (Q/4\pi) \ln [ ( (x+a)^2 + y^2 ) / ( (x-a)^2 + y^2 ) ] \quad (4)$$

219 for a source at location  $x=-a, y=0$  and a sink at location  $x=+a, y=0$ . Here,  $Q$  is the sink and source  
 220 strength given by

$$221 \quad Q = F/\varphi h \quad (5)$$

222 where  $F$  is the volume flux (m<sup>3</sup>/s),  $\varphi$  is porosity and  $h$  is layer thickness. Note that this first attempt at  
 223 quantification assumes there is no regional flow. Any strong regional flow would remove electrolyte  
 224 from the storage location and should therefore be avoided.

225 An alternate formulation (Darcy-flow of a viscous fluid through a porous medium) gives a flow  
 226 velocity of

$$227 \quad \mathbf{u} = (-k/\mu\varphi) \nabla P. \quad (6)$$

228 Here,  $k$  is permeability,  $\mu$  is viscosity and  $P$  is pressure. Comparison of eqns (3) and (6) then implies

$$229 \quad P = (-\mu\varphi/k)\Phi + P_b \quad (7)$$

230 where  $P_b$  is a background pressure. Combining eqns (4), (5) and (7) gives the excess pressure field as

$$231 \quad \Delta P = P - P_b = -( \mu F / 4\pi k h ) \ln [ ( (x+a)^2 + y^2 ) / ( (x-a)^2 + y^2 ) ]. \quad (8)$$

232 The injection pressure is the excess pressure at the injection well radius,  $r_w$ , i.e. where

$$233 \quad (x+a)^2 + y^2 = r_w^2. \quad (9)$$

234 Hence, the excess pressure around the injection well is

$$235 \quad \Delta P = -( \mu F / 4\pi k h ) \ln [ r_w^2 / ( r_w^2 - 4ax ) ]. \quad (10)$$

236 But  $r_w \ll a$  and  $x \approx -a$ . Hence,

237 
$$\Delta P = ( \mu F / 4\pi k h ) \ln[ 4a^2 / r_w^2 ].$$
 (11)

238 The key quantity in this expression is the volume-flux,  $F$ . This flux can be combined with the energy  
 239 density,  $\rho_e$ , to give the device power. This energy density is defined, for electrochemical devices, as  
 240 the maximum energy stored divided by the volume of the entire device which, for a flow-battery, is  
 241 dominated by the combined volume of the two electrolytes. Hence, rearranging eqn (11) for  
 242 volume-flux of both electrolytes combined (i.e.  $2F$ ) and introducing the energy density of the  
 243 electrolyte leads to

244 
$$\text{Power} = 2F\rho_e = 8\pi\Delta P k h \rho_e / \mu \ln[4a^2/r_w^2].$$
 (12)

245 Equation (12) is a key indicator of SFB performance. For example, a maximum safe excess pressure  
 246 of 2 MPa, a permeability of 2D ( $=1.97 \times 10^{-12} \text{ m}^2$ ), a reservoir thickness of 100m, an energy density of  
 247  $277 \text{ MJ/m}^3$  ( $= 77 \text{ Wh L}^{-1}$ , see earlier) a viscosity of  $4 \times 10^{-4} \text{ Pas}$  (appropriate for a water-based  
 248 electrolyte at 2km depth, (Likhachev 2003)), a well separation of 80 m (i.e.  $a=40\text{m}$ , see later for  
 249 justification) and a bore-radius of 0.1m gives a power of 514 MW.

250 This is encouraging. For comparison, the London Array (the world's largest offshore wind-farm when  
 251 completed in 2013) has a capacity of 630 MW. The SFB installation described above would therefore  
 252 be capable of providing back-up of 81% of the maximum output from a wind-farm of London Array  
 253 size.

254 Power-levels therefore look useful but the facility should also store sufficient energy to provide  
 255 backup over an extended period. This capacity will be controlled by the size of subsurface  
 256 containment structure and that will be site-specific. However, an order of magnitude estimate can  
 257 be obtained from the time taken for electrolyte to travel from the injection well to the extraction  
 258 well. This can be thought of as the time to "fill" or "empty" the reservoir since, after that time,  
 259 partially (or fully) charged/discharged electrolyte will start to appear at the "wrong" well. In practice,  
 260 the charge/discharge can continue beyond this point with little loss of performance since electrolyte  
 261 will also be travelling along less direct routes. Hence, the minimum travel time provides a lower-limit  
 262 for the true charge/discharge time.

263 The minimum time is found by restricting interest to the direct line between the source and sink so  
 264 that eqn. (4) simplifies to

265 
$$\Phi(x) = (Q/4\pi) \ln[ (x+a)^2 / (x-a)^2 ].$$
 (13)

266 The velocity along this line is

267 
$$u(x) = \partial\Phi / \partial x = Qa / \pi(a^2-x^2)$$
  
 268 
$$= Fa / \pi\phi h(a^2-x^2)$$
 (14)

269 giving a travel time from source to sink of

270 
$$t = \int_{-a}^a \frac{dx}{u}$$
  
 271 
$$= 4\pi\phi h a^2 / 3F.$$
 (15)

272 Substitution of  $F$ , using eqn (11), allows eqn. (15) to be expressed as

273 
$$t = (\phi\mu a^2 / 3k\Delta P) \ln[ 4a^2 / r_w^2 ].$$
 (16)

274 Equation (16) gives a charge/discharge time of 20 hours for parameter-values as before and 10%  
 275 porosity. Larger well separations increase this storage time. For example, a separation of 1 km



276 ( $\alpha=500\text{m}$ ) would provide 180 days of charge/discharge, i.e. sufficient for seasonal balancing.  
277 However, as we'll show towards the end of this paper, storage on these longer time scales is more  
278 economically achieved by storing hydrogen gas whilst SFBs are more economic at storage times  
279 similar to those from PHS.

280 The volume capacity of the resulting system is obtained from a rearrangement of eqn. (15) to yield

$$281 \quad Ft = 4\pi\phi ha^2 / 3 \quad (17)$$

282 with a corresponding energy capacity of

$$283 \quad 2Ft\rho_e = 8\pi\phi ha^2\rho_e / 3 \quad (18)$$

284 Where the factor of 2 is introduced, as before, because the system is simultaneously pumping two  
285 electrolytes. For the same parameter-values as before, equation (18) yields a capacity of 10 GWh,  
286 i.e. similar to the PHS plant at Dinorwig (see earlier).

287 The implication of these preliminary results is that SFBs could provide electricity storage with  
288 sufficient charge/discharge power and sufficient energy-capacity to be useful. In addition, SFBs have  
289 a number of possible advantages over  $\text{H}_2$  storage and CAES.

290 Firstly, the safety advantage already discussed (accidental leakage is environmentally benign) is  
291 enhanced by the near-constant storage-volume and temperature resulting from extracting charged  
292 (discharged) electrolyte whilst simultaneously injecting discharged (charged) electrolyte back into  
293 the same reservoir. This reduces the risk of containment failure since it avoids the thermo-  
294 mechanical stresses produced by the charge/discharge cycles of  $\text{H}_2$  and CAES storage (e.g. see  
295 Böttcher et al., 2017 on  $\text{H}_2$  storage in salt caverns). The negative relative pressure in the extraction  
296 half of the system also helps to maintain integrity.

297 Flow batteries can also have round-trip energy efficiencies (i.e. output energy/input energy) in  
298 excess of 80% (Tang *et al.* 2013). This compares favourably with <40% for  $\text{H}_2$  electricity storage  
299 (Pfeiffer and Bauer 2015) and ~50% for existing CAES systems (Jafarizadeh *et al.* 2020) although it  
300 should be mentioned that adiabatic CAES may allow this to increase to >60% (Hartmann *et al.* 2012).

301 However, this high efficiency would be undermined if SFBs consumed significant energy in pumping  
302 viscous electrolytes through the porous subsurface. Note that energy-loss has the same units as  $\rho_e$   
303 (i.e. energy loss for each  $\text{m}^3$  of electrolyte pumped) and should be significantly smaller than  $\rho_e$  as we  
304 do not want to consume a significant fraction of the energy stored. Note also that energy densities  
305 have units of pressure ( $\text{J}/\text{m}^3 \equiv \text{Pa}$ ) and, in fact, the pumping-loss energy density is simply the pressure  
306 drop from injection to extraction well. For the parameters used above, this is 4 MPa ( $\equiv 4 \text{ MJ}/\text{m}^3$ , due  
307 to +2Mpa at injection and -2Mpa at extraction) compared with a storage energy density of 277  
308  $\text{MJ}/\text{m}^3$ . Hence, energy loss during pumping will reduce the round-trip efficiency by less than 3% (N.B.  
309 we are pumping two electrolytes and so total losses are  $8 \text{ MJ}/\text{m}^3$ ).

310 A final theoretical advantage is the simplicity of SFBs. The same device is used for both charge and  
311 discharge and there are relatively few moving parts and no high-temperature components. Hence,  
312 SFBs are likely to be reliable, cheap to operate and relatively cheap to construct (see later for a more  
313 formal economic analysis).

314 In summary, SFBs look promising from power, storage-capacity, storage-time, safety, reliability and  
315 efficiency points of view. But these are theoretical expectations. In practice, there are significant  
316 hurdles to achieving this performance and we now turn to these.

317

## 318 Potential Problems

319 This section takes a first look at issues that may make SFBs less effective than the foregoing analysis  
320 suggests or that may make SFBs too expensive to build. We start by estimating the size of flow-  
321 battery required to achieve the performance set out in section 2. Is it unrealistically large?

322 The size of any battery is controlled by the power collected/produced by each square metre of  
323 electrode during charging/discharging (the cell power density, not to be confused with the  
324 electrolyte energy density discussed earlier). Tucker et al (2015) give a value of 180 W/m<sup>2</sup> for their  
325 all-iron flow-battery. A practical device might therefore consist of banks of, say, 1kW cells each with  
326 an electrode area of ~5m<sup>2</sup>. The thickness of each of these cells is hard to specify at present but is  
327 unlikely to differ greatly from ~0.1m to give each 1kW cell a volume of 0.56m<sup>3</sup>. Hence, the SFB  
328 described in section 2, with a power output of 514 MW, would consist of cells with a total volume of  
329 286 000 m<sup>3</sup>. This could be contained in a cube of side 66m and is similar to the enclosed volume of  
330 the superstructure of an offshore oil-rig, i.e. it's challenging but not impossible. Furthermore,  
331 electrodes can be constructed with high surface areas (e.g. hierarchically structured electrodes,  
332 (Gabardo *et al.* 2013)) and these may allow substantial reductions in cell volume.

333 Higher power densities may also be possible. Gong et al. (2016) report all-iron flow-battery power  
334 densities of up to 1.6 kW/m<sup>2</sup> when using triethanolamine and cyanide anions in place of Cl<sup>-</sup>.  
335 Unfortunately, these alternate anions have significant cost and environmental disadvantages and  
336 the order-of-magnitude improvement in volume only reduces device linear dimensions by a factor of  
337 two.

338 Another relevant factor is the possible need to cool the cells. This could require pumping of coolant  
339 with consequent increases in device volume and complexity. Fortunately, this does not appear to be  
340 an issue. If we assume the energy losses occur as low-grade heat which warms the electrolyte, then,  
341 from the definition of specific heat capacity,  $c$ , the expected warming,  $\Delta T$ , is

$$\begin{aligned} 342 \quad \Delta T &= \Delta H / cM \\ 343 \quad &= 2\rho_e F(1-\eta)t / 2cpFt \\ 344 \quad &= \rho_e(1-\eta) / cp \end{aligned} \quad (19)$$

345 where  $\Delta H$  is heat input,  $M$  is mass,  $\eta$  is efficiency, and  $t$  is time. Assuming  $\rho_e=277$  MJ/m<sup>3</sup>,  $\eta=0.9$  (10%  
346 energy losses on charging and 10% energy losses during discharging i.e. an 80% round-trip  
347 efficiency),  $c=4.2$  kJ/K/kg and  $\rho=1000$  kg/m<sup>3</sup> then gives  $\Delta T=6.6$ K. This can easily be absorbed by the  
348 electrolytes; especially as they will have cooled from their subsurface values (~60 °C for a 2 km deep  
349 reservoir) as they were pumped up from depth and into the flow-cell.

350 The next problem we consider is that the maximum rate at which electrolyte can be pumped is  
351 constrained by the physics of porous reservoirs and so, to achieve high powers, the electrolyte must  
352 have high energy density. Unfortunately, achieved values are significantly lower than theoretical  
353 ones for the all-iron design. Tucker et al. (2015), for example, only achieved a density of 11.5 Wh/L  
354 ( $\cong 41.4$  MJ/m<sup>3</sup>)—a factor of 5 less than assumed in section 2. This brings the SFB estimated power  
355 down to 77 MW which may not be high enough to make such a system economic.

356 Yu et al. (2021) achieved a significantly better energy density of 32 Wh/L ( $\cong 115$  MJ/m<sup>3</sup>), using  
357 sulphate anions in place of chlorine, but this required addition of 1-ethyl-3-methylimidazolium

358 chloride to enhance sulphate solubility. The cost and environmental implications of this requires  
359 further investigation.

360 Other ways forward, if energy densities are unavoidably low, is to increase the driving pressure  
361 and/or the reservoir permeability. There is some scope to increase pressure (e.g. by using deeper  
362 reservoirs) but this is ultimately limited by the efficiency issues discussed earlier; a 4 MPa pressure  
363 drop implies almost 20% energy losses due to pumping (if the energy density is only 41.4 MJ/m<sup>3</sup>) and  
364 this deteriorates further as pressure is increased. An alternative approach is to increase permeability  
365 using hydraulic fracturing (Valkó 2014).

366 Another way to tackle issues of low energy density is simply to sink more wells, either into the same  
367 reservoir zone or, possibly, into a number of separate electrolyte ponds. This obviously increases  
368 costs. Horizontal drilling would also increase flow rates significantly (e.g. it has been used to obtain  
369 high rates of CO<sub>2</sub> injection at Sleipner (Kongsjorden *et al.* 1998)).

370 Hence, low energy density is unlikely to be an insuperable barrier to SFB deployment. Further  
371 research may bring energy densities up (current values are well below the theoretical maximum) and  
372 use of multiple wells, horizontal drilling and hydraulic fracturing should enable significant  
373 enhancements to the pumping rates given by the simplistic, single-source, single-sink, 2D modelling  
374 of section 2.

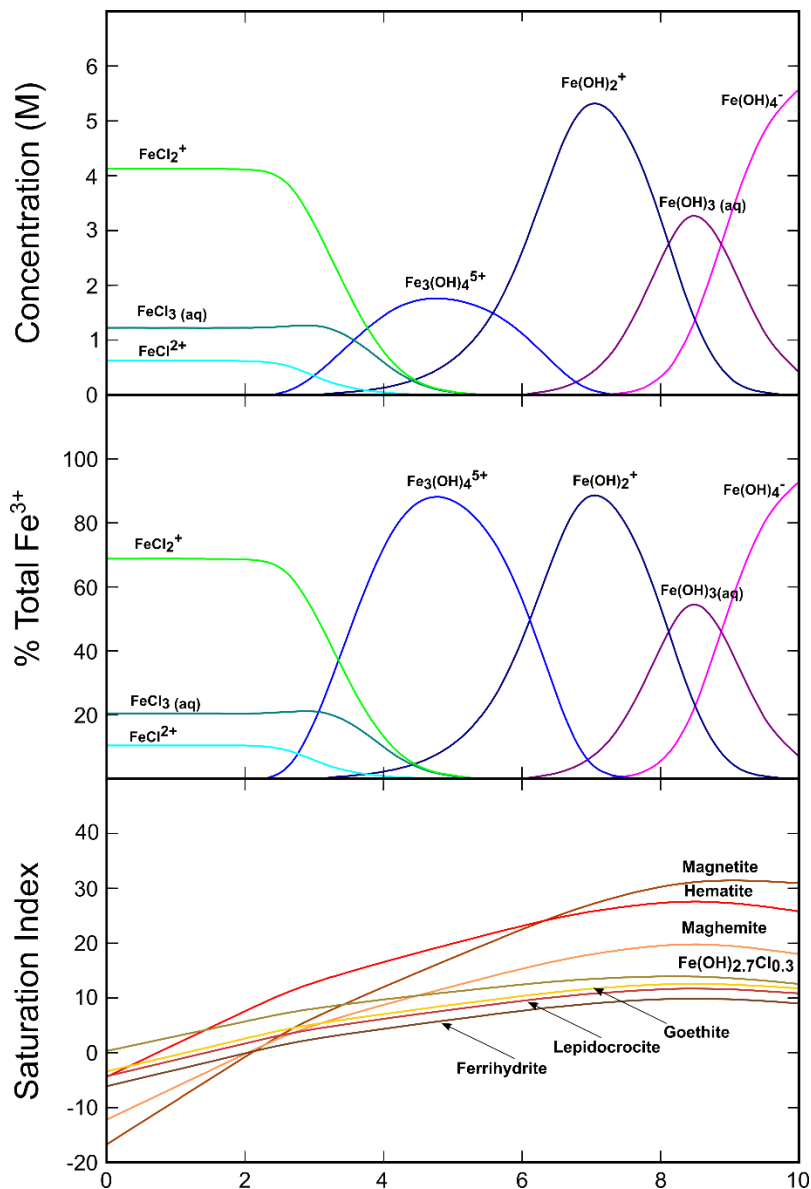
375 All the power and energy density issues, discussed to this point, will be important regardless of the  
376 flow-battery chemistry adopted. However, the all-iron configuration suffers from an additional,  
377 specific problem—“parasitic” hydrogen generation, i.e. generation of some hydrogen gas, instead of  
378 metallic iron, when reaction (2) is reversed. This reduces the round-trip efficiency of the cell but it  
379 will be suppressed by the moderately high temperature of sub-surface stored electrolyte and can be  
380 suppressed further by additives (Jayathilake *et al.* 2018). Another consequence of hydrogen  
381 production is the concomitant formation of insoluble iron hydroxide precipitate (Narayan, 2019)  
382 which may reduce reservoir permeability and which will reduce electrolyte concentration.

383 A more radical solution is to regard hydrogen generation as an opportunity rather than a problem!  
384 The SFB could be operated as a hybrid electrical-storage and H<sub>2</sub> generation device and, if a hydrogen-  
385 economy develops over the coming decades, selling parasitic hydrogen may be more cost-effective  
386 than preventing its generation. However, this would not solve the issue of iron hydroxide  
387 precipitation.

388 The subsurface nature of our proposed SFBs introduces a number of additional problems. The first is  
389 that electrolytes will inevitably be contaminated by contact with mineral surfaces, diluted by pore-  
390 fluids and metabolised by microbes in the subsurface. We need to determine whether these  
391 interactions will significantly reduce flow battery performance.

392 Some chemicals present may actually help (for example, NaCl is frequently used as a supporting  
393 electrolyte in flow batteries (e.g. Mundaray *et al.* (2021)) but other contaminants could result in  
394 unwanted side-reactions that consume reactants needed for reactions (1) and (2) or that lead to Fe  
395 loss and precipitates (e.g. iron oxides, hydroxide, and FeOOH) blocking pore-spaces and preventing  
396 electrolyte flow. However, some precipitates such as calcite or quartz may also be useful as they will  
397 predominantly form at the brine/electrolyte interface and, hence, help seal off the electrolyte from  
398 the brine. Detailed experimental investigations and geochemical modelling bringing electrolytes into  
399 contact with realistic brine chemistries and mineral surfaces will allow progress on understanding  
400 these issues.

401 Another major concern is electrolyte loss that depends on thermodynamic stability of injected  $\text{FeCl}_3$   
 402 in formations waters. Wide variations in major ion and trace element chemistry are reported for the  
 403 formation waters from the North Sea (see Warren et al., 1994) and quantifying the stability of  
 404 aqueous  $\text{FeCl}_3$  in every type of formation water is beyond the scope of this paper. Here, we illustrate  
 405 this effect using a simplified idealised composition of formation water at equilibrium with the  
 406 surrounding minerals reported from Sleipner field in the North Sea (Gauss et al., 2005) as this  $\text{CO}_2$   
 407 storage location may also be suitable for electrolyte storage. This formation water has a pH of 7.67  
 408 and contains  $3.5 \times 10^{-8}$  M Al,  $1.25 \times 10^{-5}$  M Ba, 0.177 M Ca, 0.479 M Cl,  $2.48 \times 10^{-7}$  M  $\text{Fe}^{2+}$ ,  $1.4 \times 10^{-4}$  M  
 409  $\text{K}^+$ , 0.011 M  $\text{Mg}^{2+}$ , 0.1 M  $\text{Na}^+$ ,  $4.5 \times 10^{-4}$  M Si, and  $2.5 \times 10^{-4}$  M sulphate at 37 °C. Assuming no redox  
 410 change and that the solution is in equilibrium with atmospheric  $\text{CO}_2$  and contains no dissolved  $\text{O}_2$ ,  
 411 we calculate the aqueous speciation of ferric iron after injection of 6 M  $\text{FeCl}_3$ .



412  
 413 Figure 3. Aqueous speciation of  $\text{Fe}^{3+}$  phases in terms of concentration (top panel) and fraction of total  $\text{Fe}^{3+}$   
 414 (middle panel) in a solution similar to formation water at Sleipner field, North Sea (Gause et al., 2005). The  
 415 concentration of  $\text{Fe}^{3+}$  is 6 M. The bottom panel shows the saturation index of iron oxide and oxy-hydroxide  
 416 minerals with pH.

417 In our calculations, the solution becomes supersaturated with Fe-oxides (magnetite, hematite,  
418 maghemite) and -oxyhydroxides (lepidocrocite, goethite, ferrihydrite) above pH ~ 2.0. These  
419 preliminary calculations show a complete loss of the injected FeCl<sub>3</sub> at near-neutral pH, at which  
420 point precipitation of Fe-oxides and -oxyhydroxides also becomes extremely likely. Furthermore,  
421 additional loss of electrolyte takes place via hydrolysis of Fe<sup>3+</sup> forming insoluble Fe(OH)<sub>3</sub>, and via  
422 adsorption of Fe<sup>3+</sup> onto mineral surfaces. In addition, when Fe speciation is calculated using a pe of -  
423 4.07 (Gauss et al., 2005), we observe a near complete loss of all Fe<sup>3+</sup> between a pH range of 0.0 and  
424 8.0. A detailed quantification of possible redox reactions relevant to North Sea formation waters is  
425 beyond the scope of this article but future models should consider the effect of redox  
426 transformation of Fe and related electrolyte loss.

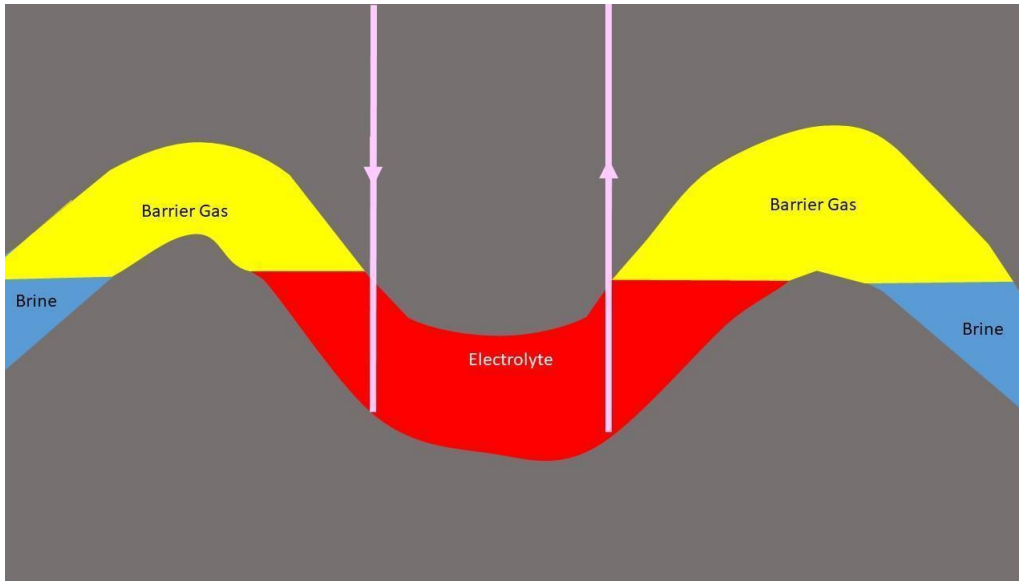
427 Microbes can also alter the electrolyte chemistry. In particular, charged electrolyte contains energy  
428 and is therefore a potential food-source (c.f. microbial contamination of stored H<sub>2</sub> (Zivar *et al.*  
429 2021)). For example, in the presence of carbon compounds many anaerobic microbial communities  
430 “feed” by converting Fe(III) to Fe(II) (Chapelle 2001). Recently, microbial communities capable of  
431 reducing Fe<sup>3+</sup> to Fe<sup>2+</sup> have been identified in an oilfield (Vigneron *et al.*, 2017). It has also been  
432 shown that naturally occurring strains of sulphur oxidising microbes can reduce aqueous FeCl<sub>3</sub> under  
433 acidic conditions (Brock and Gustafson, 1976). This would short-circuit reaction (1). We also need to  
434 consider the presence of produced hydrogen which may serve as an excellent electron donor for the  
435 microbial metabolism, alter terminal electron accepting reactions, and stimulate biomass growth in  
436 the subsurface.

437 Hence, SFBs may suffer from microbially mediated self-discharge which could substantially reduce  
438 the useful storage duration and round-trip efficiency. Experiments are needed to quantify the  
439 severity of this problem as well as the extent to which it will be ameliorated by the moderately high  
440 temperature and salinity of the electrolytes. Experiments can also be undertaken to assess the  
441 effectiveness of “cleaning” the reservoir to remove carbon compounds.

442 A final consequence of bringing concentrated electrolytes into contact with natural brines is that it  
443 will lead to dilution through diffusive loss of ions. This will result in additional self-discharge and will  
444 require the electrolytes to be repeatedly “topped up”, adding further costs. Precipitates at the  
445 brine/electrolyte interface may help prevent this problem and numerical modelling will allow its  
446 severity to be evaluated.

447 If electrolyte contamination and dilution are resistant to the solutions suggested above, they may  
448 instead be ameliorated by pre-flooding the reservoir with a non-reactive gas so that electrolytes are  
449 no longer in direct contact with native brine (Fig. 4). An exciting possibility would be to use CO<sub>2</sub> as  
450 this barrier, since SFBs could then also play a role in carbon-sequestration. The presence of CO<sub>2</sub>  
451 would also lower the pH and, hence, help to suppress the generation of precipitates discussed  
452 above. However, using a barrier gas would require the reservoir to be sealed above as well as below  
453 and this would reduce the number of suitable locations.

454 The fact that we plan to store electrolytes in porous media, rather than in well-mixed tanks, will also  
455 lead to novel problems. During charging we pump uncharged electrolyte out of one well whilst  
456 pumping-in charged electrolyte at another, spatially separate, well. The opposite happens during  
457 discharging (i.e. we reverse pumping direction so that discharged electrolyte is pumped into the  
458 uncharged electrolyte end of the reservoir). As a consequence, charged and discharged electrolytes  
459 are kept separate rather than being well mixed. Even after long-term use, there are likely to be  
460 significant ion-concentration gradients within the reservoirs.



461

462 Figure 4. Protecting the electrolyte from contamination and diffusive ion-loss using a barrier gas (e.g. CO<sub>2</sub>, N<sub>2</sub>  
 463 or naturally present CH<sub>4</sub>).

464 The consequences of this for flow-battery performance are unclear although it should help keep  
 465 relevant ions at relatively high-concentrations and hence maintain high power levels. Laboratory  
 466 experiments are needed to investigate further and we propose to set up a laboratory all-iron cell  
 467 with 4 tanks—one for charged anode electrolyte, one for discharged anode electrolyte, one for  
 468 charged cathode electrolyte and one for discharged cathode electrolyte—to determine how this  
 469 separation affects performance.

470 Porous media additionally lead to the possibility that pore-spaces could become blocked by  
 471 precipitates. This was mentioned earlier in the context of chemical contamination but precipitates  
 472 can form even if there are no unwanted side-reactions since the iron deposited in reversed reaction  
 473 (2) may not all be deposited on the electrode whilst the FeCl<sub>3</sub> involved in reaction (1) is a relatively  
 474 low-solubility compound unless we operate the electrolyte at very low pH. Once again, laboratory  
 475 work is required to evaluate the severity of these problems and to investigate possible solutions (e.g.  
 476 additives and filters).

477 Furthermore, porous-rock storage leads to flow-rates (and hence power) being strongly constrained  
 478 by electrolyte viscosity. The earlier calculations assumed that the electrolytes were sufficiently dilute  
 479 that viscosity approximately equalled that of water. However, Yu *et al.* (2021) showed that the  
 480 higher concentrations (2.2M) needed for good power (with iron sulphate electrolytes) led to a factor  
 481 of 3 increase in viscosity. If a similar viscosity increase occurs in all-iron electrolytes too then it will  
 482 reduce the power (but not the energy capacity) of the SFB by a factor of 3. Hence, we will need to  
 483 determine the optimum compromise between energy density and viscosity when determining  
 484 electrolyte concentrations. This requires further laboratory measurements.

485 A final set of problems, arising from sub-surface storage, is that the flow modelling of section 2 is  
 486 highly simplistic and needs to be replaced with more realistic approaches. Sophisticated numerical  
 487 models can investigate issues such as flow channelling (when flow becomes largely confined to a  
 488 few, high permeability routes) and electrolyte trapping in cul-de-sacs (when electrolyte goes into an  
 489 area but doesn't come out again). Both of these problems are well understood in the context of  
 490 water-flooding of oil-fields to enhance recovery (e.g. Goudarzi et al. (2016)) and we anticipate that

491 existing reservoir-modelling software will be able to investigate and evaluate the severity and impact  
492 of these problems.

493 We finish this section on potential problems with the need to obtain and retain public support.  
494 Given the oil industry's PR problems with hydraulic fracturing (Dodge and Metze 2017) and the fact  
495 that even wind-farms can be controversial (Ellis *et al.* 2007; Batel, 2020), it is likely that subsurface  
496 flow-batteries will meet resistance despite safety and environmental benefits. It is therefore  
497 necessary to discuss the technology openly and as widely as possible from an early stage. Issues that  
498 may affect acceptability relate to hydraulic fracturing, induced seismicity and contamination of  
499 ground water. Such considerations will also influence which locations are acceptable and may, for  
500 example, restrict development to offshore settings.

501

## 502 **A First Look at Cost**

503 Sub-surface flow batteries look promising. They can potentially provide high charge/discharge power  
504 for weeks to months and none of the technical challenges appear insurmountable. However, it is  
505 also important to consider whether SFBs are affordable.

506 We have neither the space nor the expertise for a full economic assessment, but we can take a first  
507 look at the energy installation cost. This is usually given in \$/kWh and expresses the price of  
508 installing a given amount of storage capacity. Li-ion batteries, for example, cost \$200/kWh to  
509 \$1260/kWh (IRENA, 2017) whilst CAES ranges over €40-110/kWh (~\$42-155/kWh) (Zakeri & Syri,  
510 2015). PHS costs vary significantly depending upon location and size but IRENA (2017) quote an  
511 average of \$25/kWh whilst Zakeri & Syri (2015) suggest €68/kWh (i.e. around \$71/kWh).

512 Hence, if SFBs are to be an affordable alternative to PHS and CAES, the energy installation cost needs  
513 to be of the order of \$50/kWh or less. We discuss the cost-comparison with hydrogen-storage in  
514 more detail a little later.

515 To estimate energy installation cost for an SFB, we use the fact that flow batteries decouple the  
516 system power from the system capacity. In traditional battery storage, both the power and the  
517 capacity are increased by adding cells whereas, in flow batteries, we increase power by adding more  
518 cells and increase capacity by adding more electrolyte. This separation of power from capacity  
519 allows the system cost to be divided into those that scale with the power (i.e. the cost of adding  
520 more or bigger stacks) and those that scale with capacity (i.e. the cost of increasing electrolyte  
521 volume).

522 For simplicity, in this first analysis, we assume that costs increase linearly with scale (as assumed also  
523 by others, e.g. see Mellentine (2011) and Yu et al (2021)). The overall installation cost is then

$$524 \quad C = C_p P + C_e E \quad (20)$$

525 where  $C$  is cost,  $C_p$  is cost per unit power (for those components whose cost scales with power),  $P$  is  
526 power,  $C_e$  is cost per unit energy (for those components whose cost scales with the energy capacity)  
527 and  $E$  is energy capacity. In other words,  $C_p$  is the cost/kW for the stack whilst  $C_e$  is the cost/kWh for  
528 the tanks plus electrolytes.

529 The energy installation cost is, by definition, then

$$530 \quad \frac{C}{E} = C_p \left( \frac{P}{E} \right) + C_e$$

531 
$$= C_p T^{-1} + C_e. \quad (21)$$

532 where T is the storage duration defined as the time to fully charge or fully discharge the SFB at  
 533 maximum power. With this background, we can investigate how well an SFB might perform  
 534 economically.

535 Mellentine (2011) has estimated costs for a 10kW, 20.9kWh all-iron flow battery and these imply a  
 536 cost for the stacks alone (i.e. without electrolytes, tanks and pumps) of \$1338/kW. Alternatively, Yu  
 537 et al (2021) put the stack cost at \$135.1/m<sup>2</sup> which, combined with Tucker et al's (2015) power  
 538 density estimate of 180W/m<sup>2</sup>, implies \$750/kW. In this section, we adopt the lowest price estimates  
 539 because economies of scale are likely to push costs down significantly when flow batteries are used  
 540 at grid-scale rather than the laboratory scale used in the papers we are getting costs from. Hence,  
 541 we set C<sub>p</sub> to \$750/kW.

542 There are two main components to C<sub>e</sub>: (i) the cost of storage tanks; (ii) the cost of electrolytes. In a  
 543 wide-ranging review of the literature, Zakeri & Syri (2015) estimate hydrogen storage costs in tanks  
 544 at \$15/kWh and in geological storage at €0.25/kWh (~\$0.26/kWh). However, the energy density of  
 545 hydrogen is higher than that for flow-battery electrolytes. Taking the hydrogen energy density as  
 546 132 kWh/m<sup>3</sup> (Kabuth et al, 2017), compared to the SFB energy density of 77 kWh/m<sup>3</sup> used  
 547 throughout this paper, implies that the storage costs will be 132/77=1.7 times higher, i.e. \$26/kWh  
 548 for surface storage and \$0.45/kWh for underground storage.

549 Moving onto the electrolytes themselves, Mellentine (2011) estimated costs, for the electrolytes  
 550 alone, at \$21/kWh. Tucker et al (2015), on the other hand, report costs of \$6.07/kWh whilst Yu et al  
 551 (2021) have an electrolyte cost of only \$3.37/kWh. As discussed above, we will use the lowest  
 552 estimate.

553 Finally, for T, we use 20 hours as calculated earlier in this paper for the proposed 513MW, 10GWh  
 554 SFB.

555 With these parameters, eqn (21) gives an energy installation cost of \$67/kWh for flow batteries with  
 556 surface tanks and \$41/kWh if electrolytes are stored in the subsurface. These are encouraging cost  
 557 estimates which would make flow battery storage about the same cost as CAES and pumped-hydro  
 558 storage but with less severe geographical limitations.

559 The analysis can be extended to give estimates of the power installation cost which is usually given  
 560 in \$/MW and expresses the price for a given charge/discharge power. This is particularly useful for  
 561 comparing to costs of generators. For example, wind-turbines currently cost around \$1-2  
 562 million/MW and, ideally, we need storage power-costs to be smaller than this so that adding storage  
 563 does not greatly increase the overall cost of wind-turbine power. As a benchmark, Zakeri and Syri  
 564 (2015) estimate the power installation cost for PHS at €1.40 million/MW (~\$1.46 million/MW).

565 From eqn (20), the power installation cost is

566 
$$\frac{C}{P} = C_e \left( \frac{E}{P} \right) + C_p$$

567 
$$= C_e T + C_p \quad (22)$$

568 which, with the parameters given above, yields a cost of \$1.3 million/MW for a system with surface  
 569 tanks and \$0.8 million/MW for subsurface storage. Hence, the power installation cost also looks  
 570 promising.



571 A similar analysis to that above can be carried out for hydrogen storage to allow a direct comparison.  
 572 Schoenung (2011) gives the relevant figures for a hydrogen-based power to gas system as \$340/kW  
 573 for the electrolyser, \$500/kW for the fuel cell (hence  $C_p$ =\$840/kW, a little higher than for SFBs) and  
 574 \$0.3/kWh (much lower than for SFBs) for underground storage ( $=C_e$  since the cost of water can be  
 575 assumed negligible).

576 The broad outline of this comparison is unlikely to change substantially as a consequence of future  
 577 technical developments. Specifically,  $C_p$  will likely remain lower for SFBs than for H<sub>2</sub> because the  
 578 latter approach requires both an electrolyser and a fuel-cell (or gas turbine) whereas energy storage  
 579 and recovery are achieved using a single device in SFBs. The technologies behind electrolysers, fuel-  
 580 cells and flow-batteries are similar and so  $C_p$  for SFB storage might conceivably become as little half  
 581 the value for H<sub>2</sub> storage but is unlikely to get much smaller than that. In contrast,  $C_e$  will always be  
 582 lower for H<sub>2</sub> storage than for SFB storage since the “feedstock” for H<sub>2</sub> storage is water at negligible  
 583 cost. In addition, storage costs will always be lower for high-energy-density H<sub>2</sub> than for lower-  
 584 energy-density electrolytes. Hence, we can be moderately confident that  $C_{pf} < C_{ph}$  and  $C_{eh} < C_{ef}$  will not  
 585 change in the future (where  $C_{ph}$  is  $C_p$  for hydrogen storage,  $C_{pf}$  is  $C_p$  for flow battery storage,  $C_{ef}$  is  $C_e$   
 586 for flow battery storage and  $C_{eh}$  is  $C_e$  for hydrogen storage).

587 A consequence of this price structure is that there will be a storage duration below which SFB  
 588 storage is cheaper than H<sub>2</sub> storage (or, equivalently, a storage duration above which H<sub>2</sub> storage will  
 589 be cheaper than SFBs). The cross-over value of  $T$  can be found from either eqn (21) or (22) (which  
 590 implies that the cross-over is identical for the energy installation price and the power installation  
 591 price) and is given by

$$592 \quad T = \frac{C_{ph} - C_{pf}}{C_{ef} - C_{eh}}. \quad (23)$$

593 Using the parameters given above, this predicts a cost-advantage for SFBs for  $T < 26$  hours. At the  
 594 cross-over the energy installation prices are \$33/kWh and the power installation costs are \$0.85  
 595 million/MW, i.e. highly competitive with pumped hydroelectric storage.

596 Plausible improvements in SFB costs could take the cross-over  $T$  up to around 10-days but it is hard  
 597 to envisage price-changes that could push the threshold much higher. It is therefore inevitable that  
 598 H<sub>2</sub> storage will be economically advantaged for longer duration applications but SFBs could be  
 599 superior for applications requiring storage times of less than a few days. In terms of the storage  
 600 benefits listed in Table 1, SFBs are most likely to be useful for peaker replacement and for  
 601 congestion management.

602

## 603 **Conclusions and Future Work**

604 The first-approximation assessments made in this paper suggest that subsurface flow batteries  
 605 (SFBs) may be able to provide safe electrical storage at high-power and low-cost. The costs are likely  
 606 to be similar to those of CAES and PHS but with fewer geographical restrictions. Costs are also likely  
 607 to be lower than for hydrogen-based power-to-gas storage in applications requiring storing less than  
 608 a few-days of power. The SFB concept therefore warrants further investigation.

609 These further investigations should focus upon the following points:

- 610 1. Improved performance of flow batteries by, for example, investigating additives, alternate  
 611 chemistries and novel electrode and membrane designs. We also need to better understand  
 612 the impact on performance of not having well-mixed storage tanks. Finally, we need

- 613 understand better how to optimize the concentration-controlled trade-off between  
614 electrolyte viscosity and electrolyte energy density.
- 615 2. Improved understanding of subsurface flow. How do we maximize electrolyte flow rates and  
616 minimize electrolyte loss into the surroundings? In particular, we need to model the effects  
617 of horizontal drilling, hydrofracturing and investigate alternate geological settings (e.g.  
618 fluvial channels rather than the massive sandstones assumed in the current paper).
- 619 3. Perhaps the most critical issues are around the chemical and biological interactions with the  
620 subsurface environment. How do we minimize precipitate formation and biological  
621 interference without using highly acidic electrolytes and/or expensive additives? For  
622 example, would deeper storage (i.e. at higher temperature) help?
- 623 4. It is also important to understand better how storage needs are likely to develop over the  
624 coming decades as grids become more renewables-intense. Will the biggest unmet need be  
625 for cost-effective storage on timescales of hours, days, weeks or months? Where should  
626 storage be located geographically (near to generators, near to consumers or both)? How  
627 well would SFBs satisfy these needs?

628

629

#### 630 **Author contributions**

631 **DW:** Conceptualization (equal), formal analysis (lead), methodology (equal), original draft (lead),  
632 review and editing (equal), project administration (lead); **KH:** conceptualization (equal),  
633 methodology (equal), review and editing (equal); **AB:** conceptualization (equal), methodology  
634 (equal), review and editing (equal); **SK:** conceptualization (equal), methodology (equal), review and  
635 editing (equal); **NL:** formal analysis (supporting), review and editing (equal).

636

#### 637 **Data Availability Statement**

638 Data sharing is not applicable to this article as no datasets were generated or analysed during the  
639 current study.

640

641

642 **References**

- 643 Batel, S., 2020. Research on the social acceptance of renewable energy technologies: Past, present  
644 and future. *Energy Research & Social Science*, **68**, <https://doi.org/10.1016/j.erss.2020.101544>.
- 645 Böttcher, N., Görke, U.-J., Kolditz, • Olaf and Nagel, T. 2017. Thermo-mechanical investigation of salt  
646 caverns for short-term hydrogen storage. *Environmental Earth Sciences*, **76**,  
647 <https://doi.org/10.1007/s12665-017-6414-2>.
- 648 Chapelle, F. 2001. Ground-water microbiology and geochemistry. 477.
- 649 Deane, J.P., Ó Gallachóir, B.P. and McKeogh, E.J. 2010. Techno-economic review of existing and new  
650 pumped hydro energy storage plant. *Renewable and Sustainable Energy Reviews*, **14**, 1293–  
651 1302, <https://doi.org/10.1016/J.RSER.2009.11.015>.
- 652 Dodge, J. and Metze, T. 2017. Hydraulic fracturing as an interpretive policy problem: lessons on  
653 energy controversies in Europe and the U.S.A.  
654 <http://dx.doi.org/10.1080/1523908X.2016.1277947>, **19**, 1–13,  
655 <https://doi.org/10.1080/1523908X.2016.1277947>.
- 656 Ellis, G., Barry, J. and Robinson, C. 2007. Many ways to say ‘no’, different ways to say ‘yes’: Applying  
657 Q-Methodology to understand public acceptance of wind farm proposals.  
658 <https://doi.org/10.1080/09640560701402075>, **50**, 517–551,  
659 <https://doi.org/10.1080/09640560701402075>.
- 660 EWE. 2017. EWE plans to build the world’s largest battery | EWE  
661 [AGhttps://www.ewe.com/en/media/press-releases/2017/06/ewe-plans-to-build-the-worlds-](https://www.ewe.com/en/media/press-releases/2017/06/ewe-plans-to-build-the-worlds-largest-battery-ewe-ag)  
662 [largest-battery-ewe-ag](https://www.ewe.com/en/media/press-releases/2017/06/ewe-plans-to-build-the-worlds-largest-battery-ewe-ag).
- 663 Gabardo, C.M., Zhu, Y., Soleymani, L. and Moran-Mirabal, J.M. 2013. Bench-Top Fabrication of  
664 Hierarchically Structured High-Surface-Area Electrodes. *Advanced Functional Materials*, **23**,  
665 3030–3039, <https://doi.org/10.1002/ADFM.201203220>.
- 666 Gong, K., Xu, F., Grunewald, J.B., Ma, X., Zhao, Y., Gu, S. and Yan, Y. 2016. All-Soluble All-Iron  
667 Aqueous Redox-Flow Battery. *ACS Energy Letters*, **1**, 89–93,  
668 <https://doi.org/10.1021/ACSENERGYLETT.6B00049>.
- 669 Goudarzi, A., Delshad, M. and Sepehrnoori, K. 2016. A chemical EOR benchmark study of different  
670 reservoir simulators. *Computers & Geosciences*, **94**, 96–109,  
671 <https://doi.org/10.1016/J.CAGEO.2016.06.013>.
- 672 Hartmann, N., Vöhringer, O., Kruck, C. and Eltrop, L. 2012. Simulation and analysis of different  
673 adiabatic Compressed Air Energy Storage plant configurations. *Applied Energy*, **93**, 541–548,  
674 <https://doi.org/10.1016/J.APENERGY.2011.12.007>.
- 675 Hruska, L.W. and Savinell, R.F. 1981. Investigation of Factors Affecting Performance of the Iron-  
676 Redox Battery. *Journal of The Electrochemical Society*, **128**, 18,  
677 <https://doi.org/10.1149/1.2127366>.
- 678 Huneke, F., Linkenheil, C.P. and Niggemeier, M. 2017. *KALTE DUNKELFLAUTE ROBUSTHEIT DES*  
679 *STROMSYSTEMS BEI EXTREMWETTER*.
- 680 IEA, 2009. Prospects for Large-Scale Energy Storage in Decarbonised Power Grids. International  
681 Energy Agency, <https://www.osti.gov/etdeweb/servlets/purl/21248888>.
- 682 IEA. 2020. Projected Costs of Generating Electricity 2020. International Energy Agency,  
683 <https://www.iea.org/reports/projected-costs-of-generating-electricity-2020>.

684 IRENA, 2017. Electricity Storage and Renewables: Costs and Markets to 2030. International  
685 Renewable Energy Agency, [https://www.irena.org/-](https://www.irena.org/-/media/Files/IRENA/Agency/Publication/2017/Oct/IRENA_Electricity_Storage_Costs_2017.pdf)  
686 [/media/Files/IRENA/Agency/Publication/2017/Oct/IRENA\\_Electricity\\_Storage\\_Costs\\_2017.pdf](https://www.irena.org/-/media/Files/IRENA/Agency/Publication/2017/Oct/IRENA_Electricity_Storage_Costs_2017.pdf).

687 Jafarizadeh, H., Soltani, M. and Nathwani, J. 2020. Assessment of the Huntorf compressed air energy  
688 storage plant performance under enhanced modifications. *Energy Conversion and Management*,  
689 **209**, 112662, <https://doi.org/10.1016/J.ENCONMAN.2020.112662>.

690 Jayathilake, B.S., Plichta, E.J., Hendrickson, M.A. and Narayanan, S.R. 2018. Improvements to the  
691 Coulombic Efficiency of the Iron Electrode for an All-Iron Redox-Flow Battery. *Journal of The*  
692 *Electrochemical Society*, **165**, A1630, <https://doi.org/10.1149/2.0451809JES>.

693 King Hubbert, M. 1957. (Print) (Online) Journal homepage: <https://www.tandfonline.com/loi/thsj18>  
694 DARCY'S LAW AND THE FIELD EQUATIONS OF THE FLOW OF UNDERGROUND FLUIDS.  
695 *Hydrological Sciences Journal*, **2**, 23–59, <https://doi.org/10.1080/02626665709493062>.

696 Kongsjorden, H., Karstad, O. and Torp, T.A. 1998. Saline aquifer storage of carbon dioxide in the  
697 Sleipner project. *Waste Management*, **17**, 303–308, [https://doi.org/10.1016/S0956-](https://doi.org/10.1016/S0956-053X(97)10037-X)  
698 [053X\(97\)10037-X](https://doi.org/10.1016/S0956-053X(97)10037-X).

699 Likhachev, E.R. 2003. Dependence of Water Viscosity on Temperature and Pressure. *Translated from*  
700 *Zhurnal Tekhnicheskoe Fiziki*, **48**, 135–136.

701 Mundaray, E., Sáez, A., Solla-Gullón, J. and Montiel, V. 2021. New insights into the performance of  
702 an acid-base electrochemical flow battery. *Journal of Power Sources*, **506**, 230233,  
703 <https://doi.org/10.1016/J.JPOWSOUR.2021.230233>.

704 Munz, I.A., Johansen, H., Huseby, O., Rein, E. and Scheire, O. 2010. Water flooding of the Oseberg  
705 Øst oil field, Norwegian North Sea: Application of formation water chemistry and isotopic  
706 composition for production monitoring. *Marine and Petroleum Geology*, **27**, 838–852,  
707 <https://doi.org/10.1016/J.MARPETGEO.2009.12.003>.

708 Narayan, S., Nirmalchandar, A., Murali, A., Yang, B., Hooper-Burkhardt, L., Krishnamoorthy, S. and  
709 Surya Prakash, G., 2019. Next-generation aqueous flow battery chemistries. *Current Opinion in*  
710 *Electrochemistry* **18**, 72-80.

711 Park, M., Ryu, J., Wang, W. and Cho, J. 2016. Material design and engineering of next-generation  
712 flow-battery technologies. *Nature Reviews Materials* 2016 2:1, **2**, 1–18,  
713 <https://doi.org/10.1038/natrevmats.2016.80>.

714 Pfeiffer, W.T. and Bauer, S. 2015. Subsurface Porous Media Hydrogen Storage – Scenario  
715 Development and Simulation. 1876–6102, <https://doi.org/10.1016/j.egypro.2015.07.872>.

716 Renewable Energy Agency, I. 2017. ELECTRICITY STORAGE AND RENEWABLES: COSTS AND MARKETS  
717 TO 2030.

718 RWE. 2020. RWE researches large-scale storage for green electricity in salt  
719 caverns [https://www.rwe.com/en/press/rwe-gasstorage-west-gmbh/2020-09-30-rwe-](https://www.rwe.com/en/press/rwe-gasstorage-west-gmbh/2020-09-30-rwe-researches-large-scale-storage-for-green-electricity-in-salt-caverns)  
720 [researches-large-scale-storage-for-green-electricity-in-salt-caverns](https://www.rwe.com/en/press/rwe-gasstorage-west-gmbh/2020-09-30-rwe-researches-large-scale-storage-for-green-electricity-in-salt-caverns).

721 Schmidt, O., Melchior, S., Hawkes, A. and Staffell, I., 2019. Projecting the Future Levelized Cost of  
722 Electricity Storage Technologies. *Joule* **3**, 81-100.

723 Schoenung, S. M., 2011. Economic analysis of large-scale hydrogen storage for renewable utility  
724 applications. United States Department of Energy, doi:10.2172/1029796.

725 Scottish Renewables. 2016. *The Benefits of Pumped Storage Hydro to the UK*.

- 726 Tang, A., McCann, J., Bao, J. and Skyllas-Kazacos, M. 2013. Investigation of the effect of shunt current  
727 on battery efficiency and stack temperature in vanadium redox flow battery. *Journal of Power*  
728 *Sources*, **242**, 349–356, <https://doi.org/10.1016/J.JPOWSOUR.2013.05.079>.
- 729 Tucker, M.C., Phillips, A. and Weber, A.Z. 2015. All-Iron Redox Flow Battery Tailored for Off-Grid  
730 Portable Applications. *ChemSusChem*, **8**, 3996–4004, <https://doi.org/10.1002/CSSC.201500845>.
- 731 Valkó, P. 2014. Hydraulic Fracturing. *Kirk-Othmer Encyclopedia of Chemical Technology*, 1–24,  
732 <https://doi.org/10.1002/0471238961.HYDRVALK.A01>.
- 733 Vigneron, A., Alsop, E. B., Lomans, B. P., Kyrpides, N. C., Head, I. M., and Tsesmetzis, N., 2017.  
734 Succession in the petroleum reservoir microbiome through an oilfield production lifecycle. *The*  
735 *ISME Journal*, 11, 2141-2154. <https://doi.org/10.1038/ismej.2017.78>.
- 736 Warren, E. A., Smalley, C. P., and Howarth, R. J., 1994. Part 4: Compositional variations of North Sea  
737 formation waters. Geological Society, London, Memoirs, 15, 119-208.  
738 <https://doi.org/10.1144/GSL.MEM.1994.015.01.05>
- 739 Weber, a., Mench, M., Meyers, J., Ross, P., Gostick, J and Liu, Q., 2011. Redox flow batteries: a  
740 review. *J. Appl, Electrochem* **41**, DOI 10.1007/s10800-011-0348-2.
- 741 Yang, C-J., 2016. Pumped Hydroelectric Storage. *Storing Energy*, Letcher, T.M. (ed), Elsevier, 25-38.
- 742 Yu, S., Yue, X., Holoubek, J., Xing, X., Pan, E., Pascal, T. and Liu, P. 2021. A low-cost sulfate-based all  
743 iron redox flow battery. *Journal of Power Sources*, **513**, 230457,  
744 <https://doi.org/10.1016/J.JPOWSOUR.2021.230457>.
- 745 Zakeri. B. and Syri, S., 2015. Electrical energy storage systems: A comparative life cycle cost analysis.  
746 *Renewable and Sustainable Energy Reviews*, **42**, 569-596.
- 747 Zivar, D., Kumar, S. and Foroozesh, J. 2021. Underground hydrogen storage: A comprehensive  
748 review. *International Journal of Hydrogen Energy*, **46**, 23436–23462,  
749 <https://doi.org/10.1016/J.IJHYDENE.2020.08.138>.